Gradientless temperature-driven rotating motor from a double-walled carbon nanotube

2014 Nanotechnology 25 505701

(http://iopscience.iop.org/0957-4484/25/50/505701)

IOP Publishing Nanotechnology
Nanotechnology **25** (2014) 505701 (6pp) doi:10.1088/0957-4484/25/50/505701

Gradientless temperature-driven rotating motor from a double-walled carbon nanotube

K Cai[1], Y Li[1], Q H Qin[2] and H Yin[1]

[1] College of Water Resources and Architectural Engineering, Northwest A&F University, Yangling, 712100, People's Republic of China
[2] Research School of Engineering, the Australian National University, Acton, ACT 2601, Australia

E-mail: Qinhua.qin@anu.edu.au and caikun1978@163.com

Received 16 August 2014, revised 25 September 2014
Accepted for publication 29 September 2014
Published 25 November 2014

Abstract

Rotation of the inner tube in a double-walled carbon nanotube (DWCNT) system with a fixed outer tube is investigated and found to be inducible by a relatively high uniform temperature (say, 300 K). We also found the mechanism of a gradientless temperature-driven rotating motor lies in the inner tube losing its geometric symmetry in a high-temperature field. This mechanism can be taken as a guide for designing a motor from such a bi-tube system. Using a computational molecular dynamics (CMD) approach and the adaptive intermolecular reactive empirical bond order (AIREBO) potential, the dynamic behavior of a bi-tube system subjected to uniformly distributed temperature is studied. In particular, the effects of environmental temperature, boundary conditions of the outer tube, and intertube gap on the dynamic behavior of the bi-tube system are investigated. Numerical examples show that a bi-tube system with the inner tube having 0.335 nm of interlayer gap produces the highest rotational speed.

Keywords: carbon nanotube, molecular dynamics, molecular motor

1. Introduction

Because of their ultra-high mechanical property (induced by strong covalent bonds) within each individual tube and the ultra-low interaction between adjacent tubes (due to van der Waals interactions) [1–3], multiwall carbon nanotubes (MWCNTs) have been considered important candidates as building blocks for the next generation of nano-electro-mechanical systems (NEMS) and many types of nanodevices [4–10]. In particular, the coaxial structure of a MWCNT restricts its translational and rotational motion with only a few degrees of freedom (DOFs), making MWCNTs the key component for the fabrication of nanotube-based switches, rotors, and mass conveyors [11].

As indicated in [11, 12], for a double-walled carbon nanotube (DWCNT), the track of motion is determined by the mutual atomic interaction between inner and outer tubes. Motion types are affected by configurations of atoms in a nanotube, defined by its chirality, and commensurate/incommensurate combinations of two coaxial nanotubes. Furthermore, the track of motion follows energy minima that can consist of helical orbits ranging from pure rotation to pure translation. This flexibility of the energy surface for motion provides the framework to explore various motion-related phenomena of MWCNTs at nanoscale, such as vanishingly small friction and thermal-gradient-induced motion.

Regarding thermal-gradient-induced motion, Schoen *et al* [13, 14] simulated the thermophoretic motion of gold nanoparticles inside a CNT with a thermal gradient on the tube. Under the driving force induced by a thermal gradient of 0.2–4 K nm^{-1}, the drift velocity of nanoparticles was very low: ~0.01–0.03 m s^{-1}. Their results showed that the chirality of CNT influences the velocity of nanoparticles. Barreiro *et al* [11] experimentally confirmed that the atomic interaction between nanotubes generated distinct kinds of motion, namely rotation and/or translation along the nanotube axis, and showed that the motion was driven by a thermal gradient that generated a phononic current in one nanotube that hit and dragged the second tube. Zambrano [15] proposed a thermal-gradient-driven molecular linear motor based on DWCNTs.

In his model, the outer tube is long and the inner tube is short and capsule-like. With a thermal gradient on the outer tube, thermophoretic force drives the motion of the inner tube within the outer tube. A similar problem of a DWCNT-based motor driven by a thermal gradient was also investigated by Santamaría-Holek *et al* [16]. Using a molecular dynamics simulation, Hou *et al* [17] investigated the relationship between thermal driving force and a thermal gradient in a DWCNT with two fixed ends of the inner tube. They concluded that 'the driving force is approximately proportional to the temperature gradient, but not sensitive to the environmental temperature'. Their results also imply that the force increases to a near constant when the length of outer tube is increased to 5 nm. A critical temperature is also suggested, such that a system temperature higher than the critical temperature leads to random motion of the inner tube, but if the system temperature is lower than the critical temperature, the motion of the inner tube can be directly controlled. Rurali and Hernández [18] numerically simulated the thermophoretic motion of the buckminsterfullerene inside a single walled carbon nanotube (SWCNT) with a thermal gradient. Shenai *et al* [19] drew the profile of interaction energy between two tubes of a DWCNT subjected to a thermal gradient. They implied that the thermophoretic motion of the outer tube along the inner tube could be driven by the energy gradient induced by a thermal gradient.

Clearly, for a linear bi-tube motor, a thermal gradient on tube can produce an effective driving force for motion along the axis. However, the same thermal gradient seems to have a negligible effect on rotation along the axis of a DWCNT. That is the major reason that no work has discussed the thermal-gradient-driven rotational behavior of a DWCNT.

Besides thermal-gradient-driven motion, Tu and Ou-Yang [20] modelled a DWCNT to study its potential as a thermal ratchet. They showed that if the axial movement of the outer tube was prevented, the system in a thermal bath exhibited directional rotation when the temperature varied with time. Zhang *et al* [21] discussed the possible rotational behavior of a DWCNT bearing at the temperature of 300 K. Guo *et al* [22] investigated the intertube interaction of a DWCNT, and found that the edge force, which is the driving force of a CNT-based actuator, is temperature dependent. Xu *et al* [12] proposed a DWCNT-based device driven by temperature fluctuation. They simulated the thermally excited motion of DWCNTs at temperatures ranging from 10 K to 1500 K and found when temperature increased to 300 K, and 1000 K, the axial sliding of an incommensurate DWCNT was temporarily trapped due to structural distortion, where intertube rotation was activated and sliding was paused. The rotational behavior, however, was not investigated. In this study, detailed rotational behavior of a DWCNT-based rotating motor subjected to a uniform temperature fluctuation is demonstrated using molecular dynamics simulations. Indeed, environmental temperature, which contributes to the kinetic energy of the atoms, is a key issue in the thermal motion of the DWCNT [12]. It affects phonon vibration, and may thereby cause the motion mode of DWCNT motor to change between rotational and translational vibration [23, 24]. A DWCNT with a fixed outer tube at a constant environmental temperature may be also expected to behave 'magically'. In addition, Zou *et al* [25] simulated some mechanical performance of multiwalled CNTs within the period of 100 ps, in which there is no compulsory fix to degrees of freedom on the atoms of the outer tube.

2. Simulation results and discussion

In the present investigation, CMD simulation and AIREBO potential, which provide accurate treatment of the energetic, elastic, and vibrational properties of solid carbon [26], are used to study the dynamic behavior of bi-tubes due to gradientless temperature-driven force. A Nosé–Hoover heat bath at the temperatures of 8 K, 150 K, and 300 K is carried out for 400 ps of relaxation before numerical analysis of the dynamic behavior of the bi-tube system subjected to a uniform temperature change (the microcanonical NVT ensemble, where N is the total number of particles in the system, V is the system's volume, and T is the absolute temperature). After the thermal bath the inner tube is free and the outer tube is partly or fully fixed during the simulation. After relaxation, the simulation time is about 5–9 ns, and the time step for all simulations is set to be 1 fs. To improve simulation accuracy only one core is adopted in the computation. In the simulation, the temperature is still a statistical value related to atom velocity according to the state equation $m\bar{v}^2/2 = 3kT/2$, where m is the mass of an atom, $\bar{v}$ is the average velocity of the atom, k is the Bolzmann's constant, T is temperature.

The internal conformation of a DWCNT is characterized by the pair of chiral indices $(n_i, m_i)/(n_o, m_o)$, where (n_i, m_i) and (n_o, m_o) represent the chiral indices of the inner and outer tubes, respectively. Three factors influencing the dynamic behavior of inner tubes are investigated in the following simulations. They are environmental temperature, length of fixed parts of outer tubes, and intertube gaps. Five DWCNT models (figure 1) are considered, and their parameters are listed in table 1.

2.1. Effect of environmental temperature

In this subsection, the DWCNT (9, 9)/(14, 14) shown in figure 1(a) is used, where the outer tube is fully fixed on DOFs. The inner tube is free. After 400 ps of thermal bath, the dynamic behavior of the inner tube is simulated at three different environmental temperatures: 8 K, 150 K, and 300 K.

The top layer of figure 2(a) shows the position history of the mass center of the inner tube (MCIT) in simulation. As the temperature is very low (8 K), the amplitude of inner tube is very small, i.e., the position of the MCIT is very close to its initial position. Simultaneously, no rotation of the inner tube occurs along the axis of the tube (yellow line in the bottom layer in figure 2(a)). The inner tube, thus having low kinetic energy with respect to the low temperature, cannot be driven to move either translationally or rotationally along the axis.

At 150 K, the translation motion of the inner tube becomes very clear after 4000 ps (the top layer in figure 2(a)).

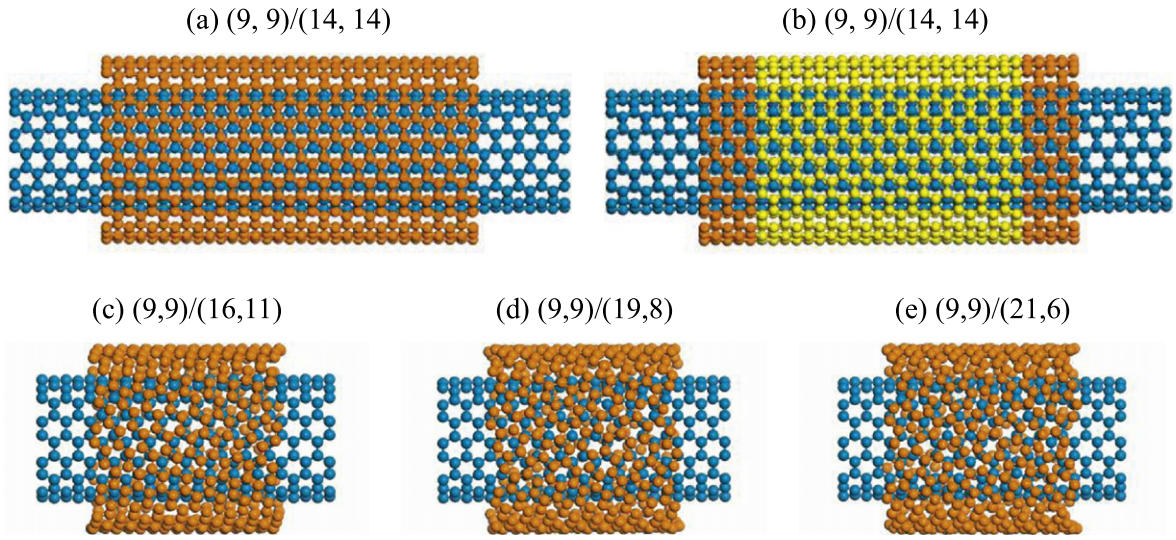

Figure 1. Five DWCNT models used in simulation (orange atoms on outer tubes are fixed on DOFs).

Table 1. Parameters of DWCNTs in figure 1.

DWCNT	Tube lengths (nm)	Intertube gap (nm)	Number of atoms
(9, 9)/(14, 14) in figures 1(a), (b)	5.986/3.991	0.343	882/924
(9, 9)/(16, 11) in figure 1(c)	2.993/1.972	0.315	450/428
(9, 9)/(19, 8) in figure 1(d)	2.993/2.011	0.335	450/442
(9, 9)/(21, 6) in figure 1(e)	2.993/2.050	0.355	450/462

At the same time, axial rotation of the inner tube is excited. However, the rotational direction varies randomly (the bottom layer in figure 2(a)). This finding implies that the inner tube cannot be used as a rotating motor at this temperature.

Dramatic phenomena are observed in the inner tube at 300 K. At that environmental temperature, the energy of the inner tube is the greatest among the three thermal conditions. Both translational and rotational motions along the axis are obvious. In particular, after 1120 ps, the rotational direction of the inner tube remains unchanged, and the rotational velocity increases almost linearly until 5830 ps. After 5830 ps, the rotational frequency of the inner tube is nearly stable, fluctuating between 56 and 63 GHz (mean value 59.5 GHz). In the study reported by Hou *et al* [17], the outer tube rotated at very low velocity. By comparing the results obtained above, **a conclusion can be drawn: the present bi-tube system at 300 K can act as a rotating motor.**

2.2. Effect of fixed lengths of outer tubes

In the following simulation, the models shown in figures 1(a), (b) are used. In total, there are 33 cross-sectional layers in the outer tube. In figure 1(b), five cross-sectional layers at each end of the outer tube are fixed after 400 ps of relaxation. The environment temperature is 300 K.

In simulation of the bi-tube system with a partly fixed outer tube, the interaction between the inner and outer tubes is lower than that of a fully fixed outer tube. Hence, stable rotation of the inner tube (with rotational frequency between 28 and 42 GHz, mean value 35 GHz) begins after 2855 ps (the bottom layer in figure 2(b)). The mean value of rotational frequency, 35 GHz, is much lower than the 59.5 GHz of the inner tube in the fully fixed outer tube. **These results indicate that a greater length of the fixed part of the outer tube leads to a higher value of rotational frequency.**

2.3. Effect of intertube gaps

To investigate the effect of the intertube gap on the rotational frequency of the inner tube in a bi-tube system with a fully fixed outer tube, the three DWCNT models shown in figures 1(c)–(e) are considered. As the equilibrium distance between two graphene sheets is about 0.335 nm, three gaps are chosen, $0.315 < 0.335$ nm, 0.335 nm and $0.355 > 0.335$ nm. After 400 ps of relaxation, simulation of 5000 ps is carried out.

From the bottom layer in figure 2(c), we see that the rotational speed of the bi-tube system in figure 1(c) (with intertube gap at 0.355 nm) is in the range 12–20 GHz after 3663 ps. The positional history of its MCIT implies that the inner tube vibrates with very small amplitude near the right end of the outer tube. We find that the inner tube in figure 1(e) (with intertube gap 0.315 nm) rotates with the rotational frequency in the range [67, 88] GHz after 1560 ps. At the same time, the translational motion of the inner tube is almost symmetric about the central cross-section of the outer tube. In comparison with the above two bi-tube systems, the inner tube in figure 1(d) (with intertube gap 0.335 nm) has the highest rotational speed of 146–173 GHz after 1670 ps. Therefore, a DWCNT with an intertube gap either greater or

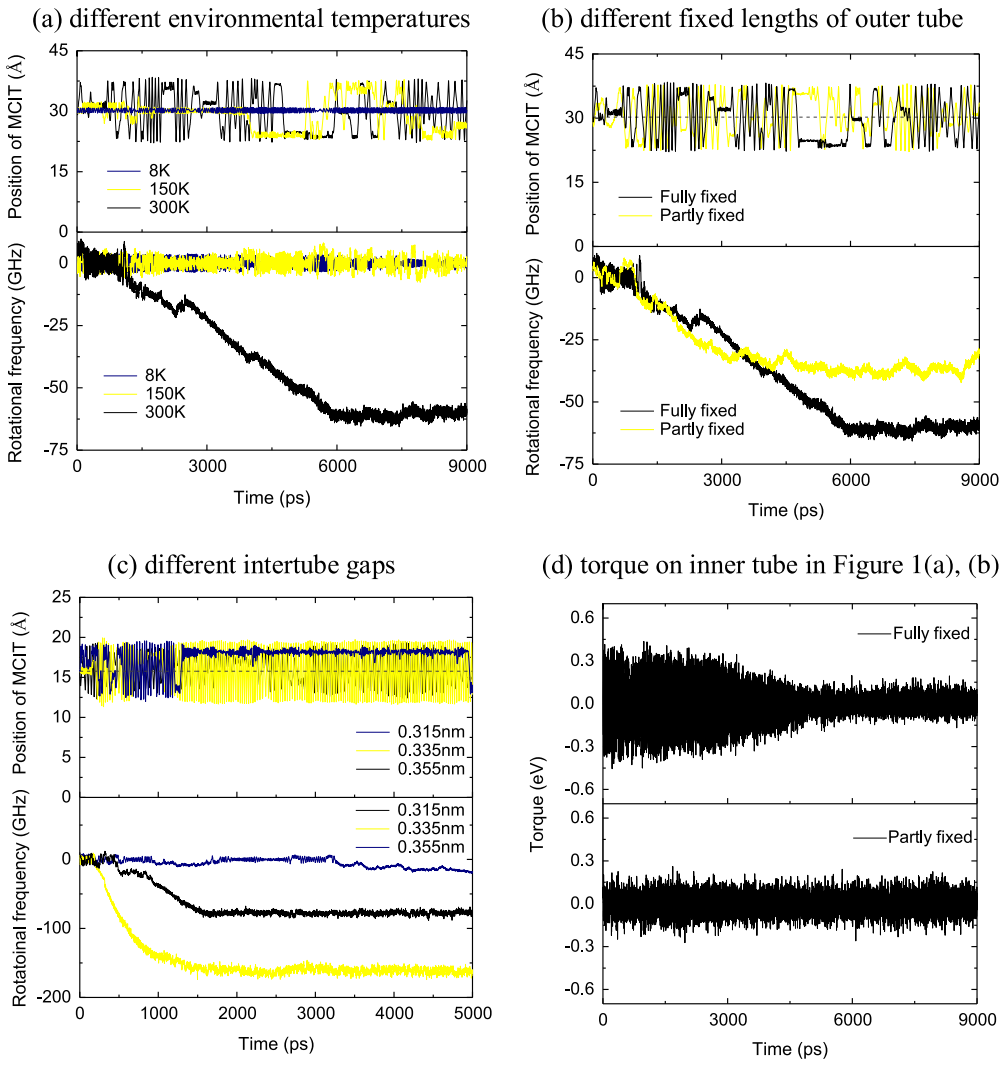

Figure 2. Translational motion and rotational motion of inner tube and torque applied on inner tube in different bi-tube systems: (a) dynamic behavior of inner tube in a bi-tube with fully fixed outer tube at different environmental temperatures, (b) dynamic behavior of inner tube in a bi-tube with fully or partly fixed outer wall at 300 K, (c) dynamic behavior of inner tubes in different outer walls with different intertube gaps at 300 K, (d) axial moment applied on inner tubes in figures 1(a), (b); the value of torque is the mean value of the torques within 1000 steps (1 ps of simulation). The dynamic behavior includes the position of the mass center of inner tube and the actual frequency of rotation of the inner tube.

less than 0.335 nm (the equilibrium distance) will have a lower rotational speed than the same inner tube in the same length of fully fixed outer tube. It is noted that, as a CNT, it can be considered as a discrete structure, and chirality difference between the inner tube and the outer tube may lead to different intertube gap [see figurea 1(c)–(e)]. We consider the intertube gap, and in turn, the chirality difference, as an intrinsic effect.

2.4. Mechanism of temperature-driven rotation

It is known that an increase in the frequency of an inner tube demonstrates that the mean value of the angular acceleration of the inner tube is either positive or negative within a period of time. Further, the angular acceleration is proportional to the torque (axial moment) applied on the inner tube, and the interactions between inner and outer tubes give rise to the torque on the inner tube. Figure 3 shows the electron density distributions of a (9,9)/(14,14) bi-tube system before and after energy minimization. Here, we find that if the whole system is axially symmetric (figure 3(a)), no torque is applied on the inner tube. But if the two tubes are relaxed (e.g., figure 3(b)) simultaneously, torque appears. However, the average value of torque in history will be close to zero and the angular acceleration of the inner tube will jump between positive and negative in simulation. Finally, the angular velocity cannot increase monotonously. Therefore, neither configuration in figure 3 can act as a rotating motor.

The DWCNT is a system with atoms distributed discretely. After relaxation, the fixed area of the outer tube (figure 1) is almost symmetric. The positions of atoms on the outer tube do not change in simulation. However, the positions of atoms on the inner tube change and the symmetry of the inner tube vanishes because of phonon vibration at high temperature. Some of the atoms in the inner tube are closer to

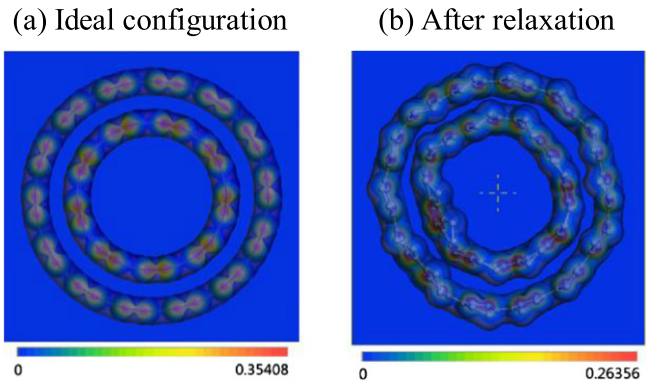

Figure 3. Electron density distributions of a three-layer DWCNT ((9, 9)/(14, 14)) before and after energy minimization.

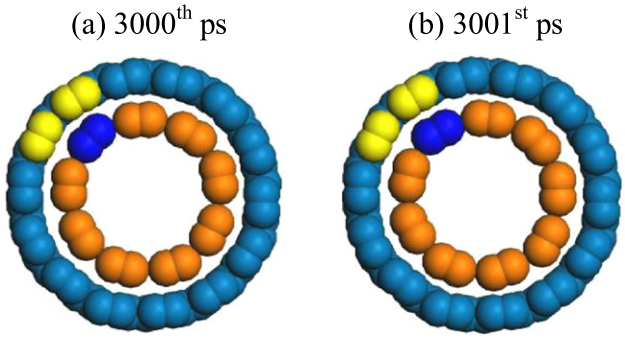

Figure 4. Configurations of a bi-tube system (with central layer of the inner tube and its two layer neighbor atoms on the outer tube) at 3000th and 3001st ps.

the outer wall and the repulsive force applied on such atoms increases sharply. Meanwhile, the symmetry of the inner tube disappears under a strong vibration state (figure 4). Both factors create the moment on the inner tube. As the DOFs of the inner tube along the axis are not constrained, accelerated rotation of the inner tube is excited by the axial moment.

Cook *et al* [2] showed that higher rotational speed lead to higher friction between two layers in a DWCNT at a constant temperature. **Hence, the rotational speed finally stabilizes when the axial moment is caused by both interlayer friction and phonon vibration being in equilibrium.**

For the inner tube, the relationship between angular velocity and torque applied by the outer tube is

$$\omega_{\text{stable}} = \int_0^{T_{\text{stable}}} M_{\text{axis}}/J_{\text{axis}}(t)\,\mathrm{d}t \qquad (1)$$

where M_{axis} is the torque (axial moment) on the inner tube and J_{axis} is the moment inertia of the inner tube along its axis. T_{stable} is the time when stable rotation of inner tube begins.

For the bi-tube systems in figures 1(a), (b), the torques shown in figure 2(d) appear to fluctuate near zero. But by calculating the summation of torques from the start to the time when stable rotation begins, we find that the total torque is −16.081 eV for the system in figure 1(a) from 0 to 5830 ps, and −7.066 eV for the bi-tube in figure 1(b) during [0, 2855] ps. Therefore, both values of M_{axis} and T_{stable} in equation (1) for the bi-tube system with a fully fixed outer tube are greater than those for the system with a partly fixed outer tube. **This is the reason the stable rotational frequency of the bi-tube with a fully fixed outer tube is higher than that with a partly fixed outer tube** (figure 2(c)).

Figure 2(c) shows that **an inner tube in an outer tube with an interlayer gap of 0.335 nm has the highest rotational speed**. The reason is that the intertube friction between two tubes with a distance less than 0.335 nm is higher than that of a bi-tube system with 0.335 nm of intertube gap if the inner tubes have the same rotational speed. If the intertube gap is greater than 0.335 nm, the interaction required between the two tubes to drive the rotation of the inner tube is lower.

3. Concluding remarks

Considering DWCNTs with fully or partly fixed outer tubes as examples, we study inner tube rotational behavior at different conditions. We find that the rotational speed of the inner tube varies with the environmental temperature, the length of the fixed part in the outer tube, and the intertube gap. A higher temperature, longer fixed sections of outer tube, and/or ∼0.335 nm of intertube gap can produce a CNT motor with a higher rotational frequency. Designing a gradientless temperature-driven rotating motor from a DWCNT is worth attempting in the manufacture of NEMS. It is also noted that phonon vibration of the inner tube can lead to asymmetric interaction between inner and outer tubes, with a moment along the axis of the bi-tube then being induced. The moment (torque) will create angular acceleration along the bi-tube's axis. The rotational speed of the inner tube increases with time.

Acknowledgments

We are grateful for partial financial support from the National Natural-Science-Foundation of China (Grant Nos. 50908190, 11372100) and the Research Foundation (GZ1205) of the State Key Laboratory of Structural Analysis for Industrial Equipment, Dalian University of Technology, China.

References

[1] Cumings J and Zettl A 2000 Low-friction nanoscale linear bearing realized from multiwall carbon nanotubes *Science* **289** 602–4
[2] Cook E H, Buehler M J and Spakovszky Z S 2013 Mechanism of friction in rotating carbon nanotube bearings *J. Mech. Phys. Sol.* **61** 652–73
[3] Qin Z, Qin Q H and Feng X Q 2008 Mechanical property of carbon nanotubes with intramolecular junctions: molecular dynamics simulations *Phys. Lett.* A **372** 6661–6
[4] Tuzun R E, Noid D W and Sumpter B G 1995 Dynamics of a laser-driven molecular motor *Nanotechnology* **6** 52–63

[5] Srivastava D 1997 A phenomenological model of the rotation dynamics of carbon nanotube gears with laser electric fields *Nanotechnology* **8** 186–92
[6] Forro L 2000 Nanotechnology—beyond gedanken experiments *Science* **289** 560–1
[7] Qiu W, Li Q, Lei Z K, Qin Q H, Deng W L and Kang Y L 2013 The use of a carbon nanotube sensor for measuring strain by micro-Raman spectroscopy *Carbon* **53** 161–8
[8] Longhurst M J and Quirke N 2007 Temperature-driven pumping of fluid through single-walled carbon nanotubes *Nano Lett.* **7** 3324–8
[9] Qiu W, Kang Y L, Lei Z K, Qin Q H and Li Q 2009 A new theoretical model of a carbon nanotube strain sensor *Chin. Phys. Lett.* **26** 080701
[10] Qiu W, Kang Y L, Lei Z K, Qin Q H, Li Q and Wang Q 2010 Experimental study of the Raman strain rosette based on the carbon nanotube strain sensor *J. Raman Spectrosc.* **41** 1216–20
[11] Barreiro A, Rurali R, Hernandez E R, Moser J, Pichler T, Forro L and Bachtold A 2008 Subnanometer motion of cargoes driven by thermal gradients along carbon nanotubes *Science* **320** 775–8
[12] Xu Z, Zheng Q-S and Chen G 2007 Thermally driven large-amplitude fluctuations in carbon-nanotube-based devices: molecular dynamics simulations *Phys. Rev.* B **75** 195445
[13] Schoen P A E, Walther J H, Arcidiacono S, Poulikakos D and Koumoutsakos P 2006 Nanoparticle traffic on helical tracks: thermophoretic mass transport through carbon nanotubes *Nano Lett.* **6** 1910–7
[14] Schoen P A E, Walther J H, Poulikakos D and Koumoutsakos P 2007 Phonon assisted thermophoretic motion of gold nanoparticles inside carbon nanotubes *Appl. Phys. Lett.* **90** 253116
[15] Zambrano H A, Walther J H and Jaffe R L 2009 Thermally driven molecular linear motors: a molecular dynamics study *J. Chem. Phys.* **131** 241104
[16] Santamaria-Holek I, Reguera D and Rubi J M 2013 Carbon-nanotube-based motor driven by a thermal gradient *J. Phys. Chem.* C **117** 3109–13
[17] Hou Q-W, Cao B-Y and Guo Z-Y 2009 Thermal gradient induced actuation in double-walled carbon nanotubes *Nanotechnology* **20** 495503
[18] Rurali R and Hernandez E R 2010 Thermally induced directed motion of fullerene clusters encapsulated in carbon nanotubes *Chem. Phys. Lett.* **497** 62–5
[19] Shenai P M, Xu Z P and Zhao Y 2011 Thermal-gradient-induced interaction energy ramp and actuation of relative axial motion in short-sleeved double-walled carbon nanotubes *Nanotechnology* **22** 485702
[20] Tu Z C and Ou-Yang Z C 2004 A molecular motor constructed from a double-walled carbon nanotube driven by temperature variation *J. Phys.: Condens. Matter* **16** 1287–92
[21] Zhang S L, Liu W K and Ruoff R S 2004 Atomistic simulations of double-walled carbon nanotubes (DWCNTs) as rotational bearings *Nano Lett.* **4** 293–7
[22] Guo Z, Chang T, Guo X and Gao H 2011 Thermal-induced edge barriers and forces in interlayer interaction of concentric carbon nanotubes *Phys. Rev. Lett.* **107** 105502
[23] Cai K, Yin H, Qin Q H and Li Y 2014 Self-excited oscillation of rotating double-walled carbon nanotubes *Nano Lett.* **14** 2558–62
[24] Falvo M R, Taylor R M, Helser A, Chi V, Brooks F P, Washburn S and Superfine R 1999 Nanometre-scale rolling and sliding of carbon nanotubes *Nature* **397** 236–8
[25] Zou J, Ji B, Feng X Q and Gao H 2006 Self-assembly of single-walled carbon nanotubes into multiwalled carbon nanotubes in water: molecular dynamics simulations *Nano Lett.* **6** 430–4
[26] Stuart S J, Tutein A B and Harrison J A 2000 A reactive potential for hydrocarbons with intermolecular interactions *J. Chem. Phys.* **112** 6472–86